A 100-kW Wireless Power Transfer System Development Using Polyphase Electromagnetic Couplers

Omer C. Onar, Gui-Jia Su, Mostak Mohammad, Veda P. Galigekere, Larry Seiber, Cliff White, Jonathan Wilkins, and Randy Wiles
Buildings and Transportation Science Division, Energy Science and Technology Directorate
Oak Ridge National Laboratory, Oak Ridge, TN

Emails: onaroc@ornl.gov, sugj@ornl.gov, mohammadm@ornl.gov, galigekerevn@ornl.gov, whitecp@ornl.gov, wilkinsjp@ornl.gov, wilesrh@ornl.gov

***Abstract*—Wireless power transfer (WPT) is an essential technology enabling automated charging of electric vehicles with safety, convenience, and flexibility while having high efficiencies. High-power wireless charging systems will be one of the dominating charging technologies for electric vehicles (EVs) in an effort to eliminate range anxiety and reduce charging times similar to that of gas station refueling practice. Polyphase electromagnetic coupler with rotating fields is a new bipolar wireless charging pad technology that can significantly increase the surface power density (kW/m2) of wireless charging coils. This study proposes a 100-kW wireless power transfer system with a compact vehicle-side (receiver) coupler that reaches to about 0.905 MW/m2 surface power density with a transmitter rated for up to 300 kW with 0.68 MW/m2. High-frequency power electronics including the inverter and rectifier designs are included in this digest along with the hardware prototype developments and preliminary experimental results.**

Keywords— polyphase coupler, wireless power transfer, electric vehicle, wireless charging.

I. Introduction

High-power charging systems are required in order to reduce the charging times of EVs to reasonable durations that can enable convenient interstate road trips without needing to wait for 8-14 hours for recharging which would be the case with Level-1 and 2 charging stations. The similar expectation exists in city driving as well for vehicle fleets providing ride-hailing/ride-sharing services as it would be impractical for those vehicles to wait for recharging in the middle of the day for multiple hours. High-power wireless charging is an attractive solution for fast charging for all types of vehicles that can automate the charging process without requiring users to handle high-power and heavy-duty cables and plugs or connectors. Similar to DC fast charging systems, WPT systems also have majority of the charging equipment offboard, which makes them more suitable for high-power applications compared to the on-board chargers.

Most of the existing WPT systems, including the high-power wireless chargers, are single-phase systems [1]-[3]. Although the use silicon carbide (SiC) -based power devices in WPT systems [4], [5] enabled higher power operations, the single-phase systems were still limited in their maximum power capabilities that is heavily restricted by the size and mass of the primary and secondary side coils. Some of those earlier developments of relatively high-power but single-phase systems include a 20-kW wireless charging system for a Toyota RAV4 EV [6] with 31.25 kW/m2 surface power density and ~95% dc-to-dc power transfer efficiency and benchtop demonstrated 100-kW system [7], [8] with about 200kW/m^2 with a dc-to-dc efficiency of >97% with a coil weight of about 50 kg. Other notable developments include a modular 65 kW IPT design with 600 mm × 600 mm transmitter and receiver pads (180 kW/m^2) [9] and the 50 kW power electronics integrated circular and DD type developments with both coil types having the same power level and dimensions with the surface power density of 160 kW/m^2 [10]. These studies are the clear indications that existing coupler geometries and designs reached out to their maximum potential in terms of the mass and size and more advanced designs must be explored.

This study proposes a polyphase wireless power transfer system with rotating magnetic fields that can achieve a more uniform magnetic field distribution allowing significantly higher space-time field utilization since there are no null points on the surface generating the magnetic field. Circular, square, rectangular, and DD type couplers have large areas on their surfaces with no contribution to the magnetic field generation. Moreover, in single-phase couplers, instantaneous power is pulsed across the airgap. With low space-time utilization, fields oscillate between zero and peak values. In polyphase design used in this study, phase windings are spatially phase shifted while the electrical excitation is also phase-shifted. As a result, each phase transfers some amount of power at a given instant while the sum of the phase powers always remains constant. Additionally, polyphase systems inherently have lower current ripples, and they allow using much smaller dc bus bar capacitors at the inverter input and rectifier output.

There have been some earlier developments of polyphase couplers for wireless charging systems. The major difference

between the proposed system and in existing studies is that previous literature either did not use rotating fields and used independently exited phase windings [11], [12] or they omitted [13] or tried to eliminate the mutual inductances between the same side phase windings since non-zero interphase mutual inductance was earlier identified as a problem in those studies [14], [15]. However, this study takes the advantage of cross-couplings between the same side phase windings. Since the phases are spatially and electrically phase shifted by 120°, that is >90°, the mutual inductances between the same side windings are negative which implies that the magnetic field from these phases add up together instead of cancelling each other. Therefore, this approach significantly increases the utilization of the coupler surface area, resulting in a higher surface power density in kW/m^2.

Some other earlier developments of multiphase systems include [16], where authors developed a four-coil WPT system with a tripolar pad-based transmitter and a single-phase receiver with non-rotating magnetic fields for up to 3.3 kW power transfer level. Magnetic modeling and simulations of a three-phase WPT system was presented in [17] with three circular unipolar coils for up to 10 kW design target. In [18], a 22-kW system is presented with a total of 12 coils with primary and secondary sides having 6 phases each. With 6 coils on each side, magnetic interference occurred between phases, which degraded the power transfer efficiency hence the interference had to be cancelled out with coupling factors that were designed such that they would result in cancellation in the voltage induced on secondary side. However, the proposed coil design in our paper has supportive magnetic fields including voltages on the secondary side that are added up instead of reduced.

The rest of this paper includes the overall system description in Section II along with development of the hardware prototypes, Section III presents the experimental results, and Section IV outlines the conclusion remarks.

II. System Description

The overall system level diagram of the proposed wireless power transfer system is presented in Fig. 1. In an effort to increase the power level of the proposed system, polyphase couplers are used in conjunction with an open-ended winding dual 3-phase inverter architecture on the primary-side. Similarly, secondary-side rectifier is also based on an open-ended winding dual 3-phase rectifier architecture. With this system, each phase winding is driven by an H-bridge inverter and each H-bridge inverter is 120° phase shifted from each other in order to achieve rotating magnetic field generation. This approach increases the power level as compared to a regular 3-phase inverter with delta (Δ) or star (Y) connected load. Both primary and secondary side couplers are compensated with an LCC resonant tuning network, similar procedure followed in [19], [20] for determining the component values. While primary-side LCC tuning provides load and coupling independent constant current behavior on primary-side coils at resonant frequency, secondary-side LCC tuning allows reduction in some of the component voltage and current stresses. As seen on Figure 1, primary side has three-phase windings that are phase A, B, and C, and secondary side also has 3 phase windings that are phase X, Y, and Z. The inductance matrix with the self-inductances of each phase windings and all the magnetic couplings between them can be defined by (1) where L_A, L_B, and L_C are the primary-side phase self-inductances, L_X, L_Y, and L_Z are the secondary-side phase self-inductances, M_{AB}=M_{BA}, M_{AC}=M_{CA}, and M_{BC}=M_{CB} are the mutual inductances between primary-side phase windings, M_{XY}=M_{YX}, M_{XZ}=M_{ZX}, and M_{YZ}=M_{ZY} are the secondary-side mutual inductances between secondary-side phase windings, and M_{AX}=M_{XA}, M_{AY}=M_{YA}, M_{AZ}=M_{ZA}, M_{BX}=M_{XB}, M_{BY}=M_{YB},

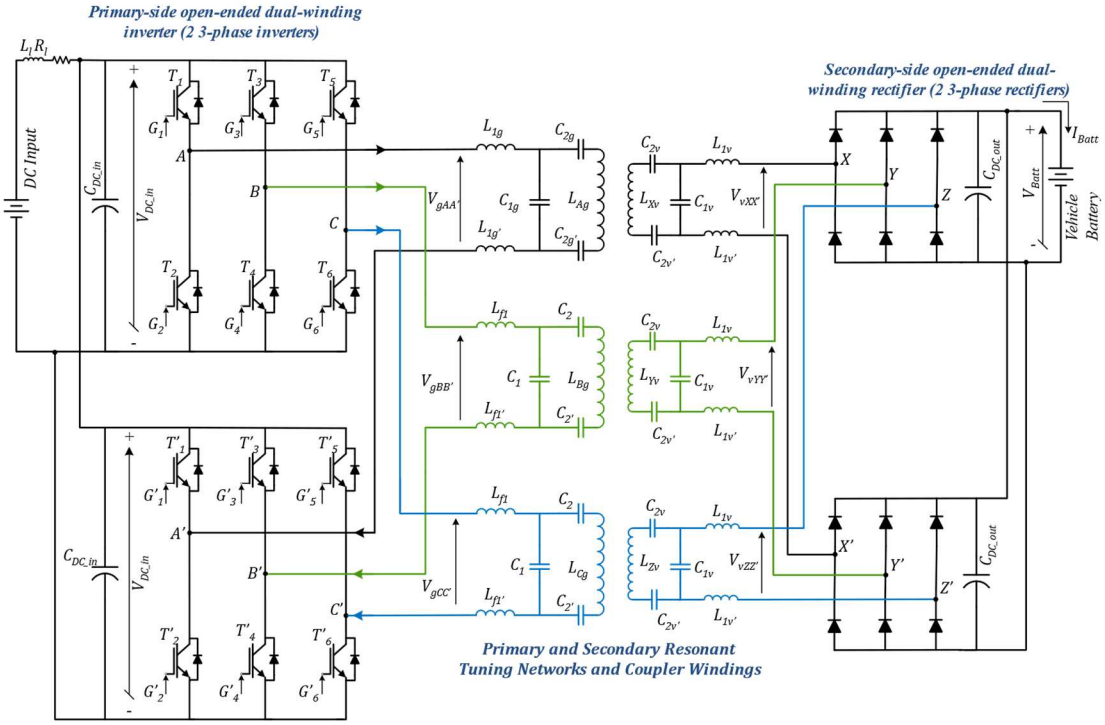

Fig. 1. System level diagram of the proposed polyphase wireless power transfer system.

M_{BZ}=M_{ZB}, and M_{CX}=M_{XC}, M_{CY}=M_{YC}, M_{CZ}=M_{ZC} are the mutual inductances between all the primary and secondary-side phase windings. The inductance matrix in (1) is diagonally symmetric under ideal conditions.

$$L = \begin{bmatrix} L_A & M_{AB} & M_{AC} & M_{AX} & M_{AY} & M_{AZ} \\ M_{BA} & L_B & M_{BC} & M_{BX} & M_{BY} & M_{BZ} \\ M_{CA} & M_{CB} & L_C & M_{CX} & M_{CY} & M_{CZ} \\ M_{XA} & M_{XB} & M_{XC} & L_X & M_{XY} & M_{XZ} \\ M_{YA} & M_{YB} & M_{YC} & M_{YX} & L_Y & M_{YZ} \\ M_{ZA} & M_{ZB} & M_{ZC} & M_{ZX} & M_{ZY} & L_Z \end{bmatrix} \quad (1)$$

Ideally, in this inductance matrix, while the mutual inductances between the phases facing each other are positive, that are M_{AX}, M_{BY}, and M_{CZ}, all the other mutual inductances are negative. Detailed system modeling derivations, input and output power expressions, and phase voltage and current equations for an LCC-LCC tuned polyphase system are provided in [21].

A. High-Frequency Inverter and Rectifier Development

The primary-side inverter hardware is shown in Fig. 2 including the engineering design and the actual hardware development. The polyphase transmitter is powered with an open-ended winding 3-phase inverters in order to utilize two 3-phase inverters while one of the inverters is connected to the phases, the other 3-phase inverter is connected on the return lines of the phases. The other way to interpret the inverter design is that each transmitter phase is driven by an H-bridge inverter.

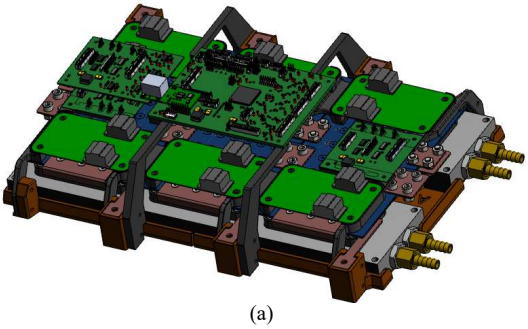

(a)

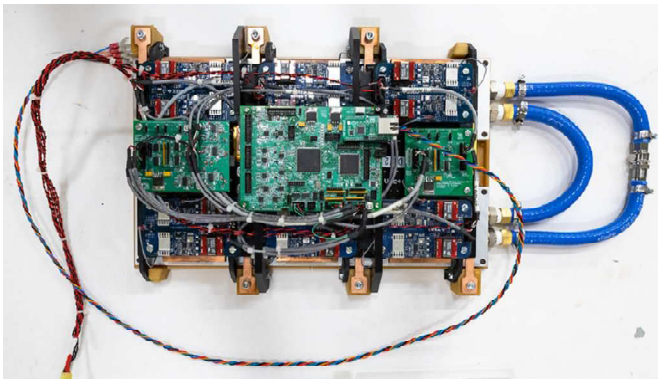

(b)

Fig. 2. Primary-side open-ended winding dual inverter: 3D engineering design (a) and completed hardware development (b).

The phase angle of $V_{AA'}$ is 0° while $V_{BB'}$ is 120° and $V_{CC'}$ is 240° to generate rotating fields with phase shifted excitation voltages. This inverter arrangement doubles the effective output voltage while maintaining dc-line capacitor size reduction compared to other options; for instance, two 3-phase inverters operated in parallel, or series cascaded multi-level inverter. This inverter uses TDK Ceralink capacitor assembly on the custom design PCB based dc bus bars that interconnects two phase-leg power modules together on a custom design heatsink fabricated by Microcool. The phase-leg power modules are 1200V/356A rated CAS325M12HM2 SiC MOSFET modules manufactured by Wolfspeed/CREE with their CGD16HB62LP gate drivers. The inverter gate signals are generated from a TMSF320F28335PGFA DSP (in the middle of the inverter in Fig. 2 (a)) from Texas Instruments with a CAN interface through a host computer for controls. Also shown in Fig. 2 (a) are the differential line drivers and receivers that convert the single-ended ePWM signals to differential signals for the gate drivers.

The rectifier for the secondary-side uses GeneSiC GB2X100MPS12-227 silicon carbide Schottky diode modules with 1200V / 200A rating at 117°C case temperature. The current rating can go up to 278A if the case temperature can be maintained at 75°C. With zero reverse recovery current and minimal forward voltage drop, a high-power and high-performance rectifier assembly is achieved in a compact size. Two diodes in the package are connected in parallel and two separate diode modules are used to form a phase-leg rectifier. One phase-leg is used for the phase winding while the other phase-leg module is connected on the return which forms open-ended winding dual rectifier assembly. Engineering drawing and the hardware development of the rectifier are shown in Fig. 3.

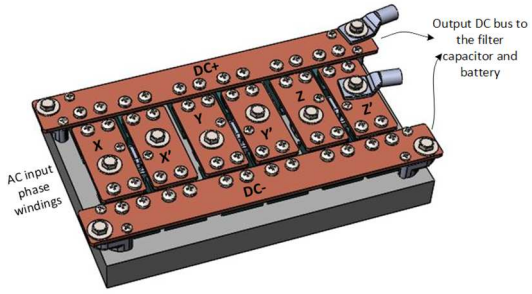

(a)

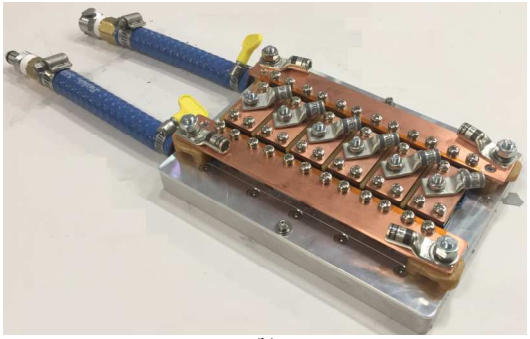

(b)

Fig. 3. Secondary-side open-ended winding dual rectifier: 3D engineering design (a) and completed hardware development (b).

B. High-Frequency Inverter and Rectifier Development

The transmitter and receiver coupler hardware developments are shown in Fig. 4 (pictures are not to the scale but diameters are indicated) while Table I shows the coil specifications. The coil geometry and design are similar to the polyphase design

described in [20] which is based on a two-layer design with 180° spatial phase-shift between the layers and 120° spatial phase-shift between the phases of each layer. Transmitter is rated for up to 300 kW (to support higher charge rates for some other vehicles) and the receiver is capable for 100 kW power level. With the given diameters, these couplers have surface power densities of 0.68 MW/m^2 for the transmitter and 0.905 MW/m^2 for the receiver.

TABLE I: COUPLER SPECIFICATIONS

Parameters	Ground Assembly (Transmitter)	100 kW Vehicle Assembly (Receiver)
Diameter	750 mm	375 mm
Litz Wire	3×4 AWG/phase	1×4 AWG/phase
Litz + Ferrite Thickness	33.6 mm (18.6+15)	28.6 mm (18.6+10)
Litz + Ferrite Mass	42.2 kg (9.9+32.3)	8.8 kg (2.4+6.4)
Worst Case Losses	2362 W (697+1665)	596 (169+311)
Coil-to-Coil Efficiency	97.4%	
Nominal airgap	152 mm	

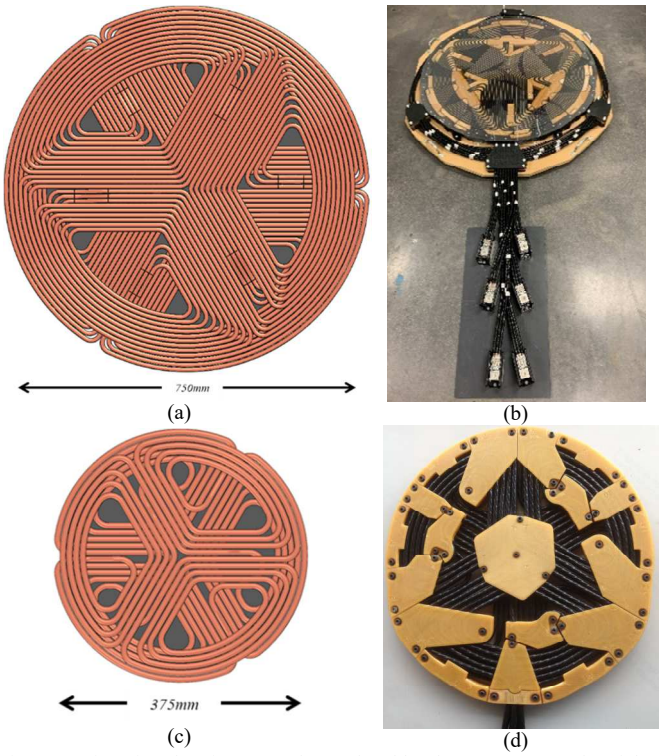

(a) (b) (c) (d)

Fig. 4. Engineering drawing (a) and completed hardware prototype (b) of the 300-kW rated transmitter and engineering drawing (c) and completed hardware prototype (d) of the vehicle-side receiver.

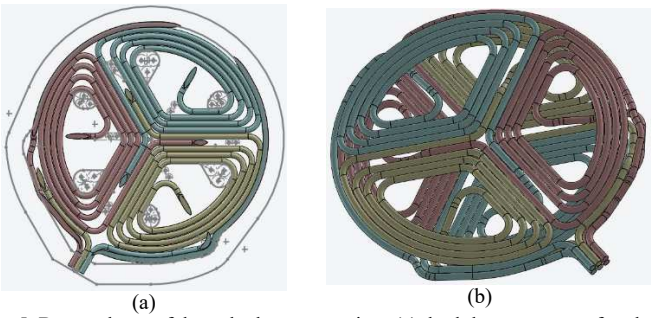

(a) (b)

Fig. 5. Bottom layer of the polyphase transmitter (a), both layers on top of each other with 180° rotational phase-shift between layers.

These couplers have two-layer structure with each layer having 3 phases and the second layer is 180° rotationally/spatially phase-shifted compared to the first layer. While Fig. 5 (a) shows the three phase windings of the first layer with different colors for each phase, Fig. 5 (b) shows both layers to better visualize the design concept.

The inductance matrix of the couplers including all the self and mutual inductances are given in (2). It should be noted that due to the random rotational positioning of the secondary coupler, phase B and Z, phase A and Y, and phase C and X are coupled with each other more effectively.

$$L = \begin{bmatrix} 14.9 & -4.22 & -4.07 & -1.67 & 1.03 & 0.23 \\ -4.22 & 15.08 & -4.12 & 0.26 & -1.6 & 1.06 \\ -4.07 & -4.12 & 14.8 & 1.13 & 0.3 & -1.52 \\ -1.67 & 0.26 & 1.13 & 15.82 & -3.93 & -3.56 \\ 1.03 & -1.6 & 0.3 & -3.93 & 15.62 & -3.48 \\ 0.23 & 1.063 & -1.52 & -3.56 & -3.48 & 15.69 \end{bmatrix} \mu H \quad (2)$$

III. EXPERIMENTAL RESULTS

The proposed polyphase wireless charging system is preliminarily tested for up to 90 kW power level (~100 kW from input) with a dc-to-dc efficiency (from input dc source to the output dc load) of 90.83% while the efficiency of the resonant stage was 97.4%. This resonant stage efficiency takes the coil-to-coil power transfer losses as well as all the losses on the primary and secondary LCC type resonant tuning components. Power analyzer recorded test results are provided in Fig. 6. Input and output dc voltages, currents, and powers, and the efficiency are shown in Fig. 6 (a) while Fig. 6 (b) shows the inverter output and rectifier input voltages, currents, and power levels for each phase along with the total inverter output power and total rectifier input power. As shown in Fig. 6 (a) inverter input voltage and current are 727.55V and 137.11A and the inverter input power is 99.749 kW while the inverter output power is 93.52 kW as shown in Fig. 6 (b). This corresponds to 93.76% efficiency on the inverter, which is relatively low. This is partially due to the slightly imbalanced inverter phase output currents that are 55.99, 52.81, and 60.98 Amps, respectively. The other reason is that the inverter input and phase output voltages are relatively high which reduces the efficiency of SiC MOSFETs. With slight adjustments on the resonant tuning inductors of the LCC network, such as adding/removing half a turn or reducing or increasing the magnetic airgap on the inductor bobbins, inverter can be moved to a more balanced condition. At the same time, resonant tuning components on primary-side can be modified to operate at lower input voltage for the same output power, to have a "close to unity" resonant voltage gain to improve the inverter efficiency further. As provided in Fig. 6 (b), rectifier input power is 91.08 kW while the rectifier output (dc load) power is 90.6 kW. This result in a rectifier efficiency of 99.47% which indicates very good performance on the vehicle-side rectifier.

The inverter output 3-phase measurements (elements 1, 2, and 3) and the rectifier input 3-phase measurements (elements 4, 5, and 6) are shown in Fig. 7 including the voltage, current, active, reactive, and apparent power levels, and the power factor and power angle.

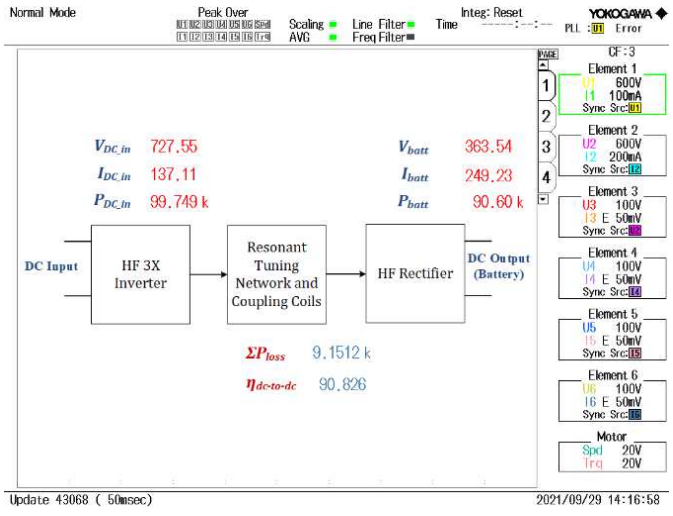

(a)

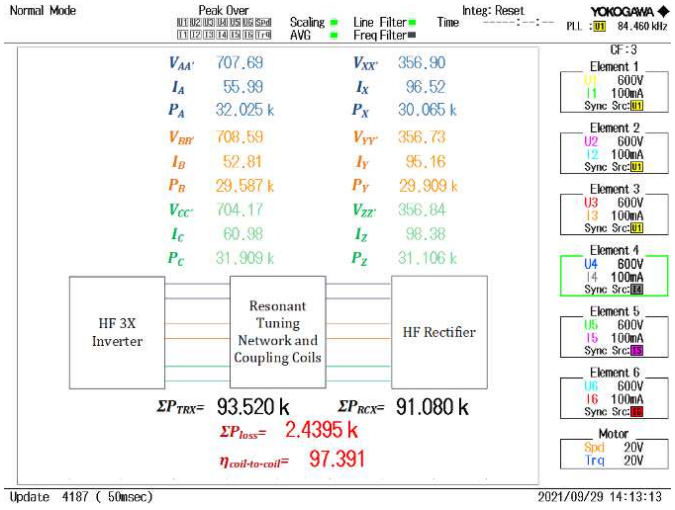

(b)

Fig. 6. Experimental results; dc-to-dc efficiency and input and output voltages and currents (a) and inverter output and rectifier input voltage, current, and power recordings (b).

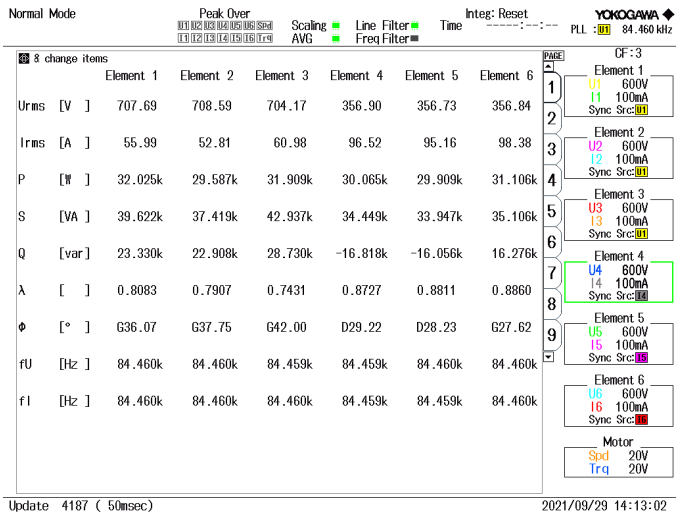

Fig. 7. Resonant stage (inverter output and rectifier input) measurements.

As shown earlier in Fig. 1, this system has four voltage and current pairs on the primary-side and four more voltage and current pairs on the secondary side. Therefore, two different 8-channel oscilloscopes are used to capture the operating waveforms of this system with an arbitrary phase-shift (timing difference) between the primary and secondary side measurements. The inverter input dc voltage and current and 3-phase output voltages and currents are shown in Fig. 8 (a) captured with an 8-channel (4 voltage and 4 current channels) Yokogawa oscilloscope while another 8-channel Teledyne Lecroy oscilloscope was used on the secondary side as shown in Fig. 8 (b). As shown on Fig. 8 (a), RMS readings of the primary-side voltages and currents are closely matching the power analyzer results shown in Fig. 6. Slight inverter output current imbalances are captured on Fig. 8 (a). Compared to the inverter phase currents, rectifier phase currents are more balanced, resulting in a higher efficiency rectifier. In addition, Fig. 8 (b) shows that the rectifier operates at near unity power factor which contributes to the high efficiency.

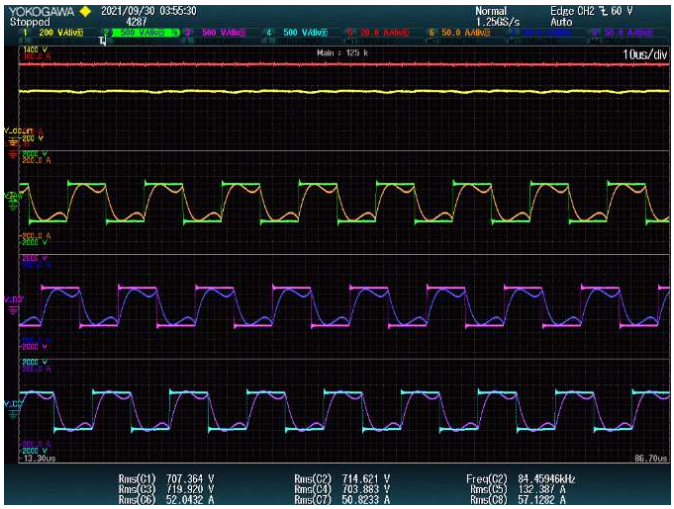

(a)

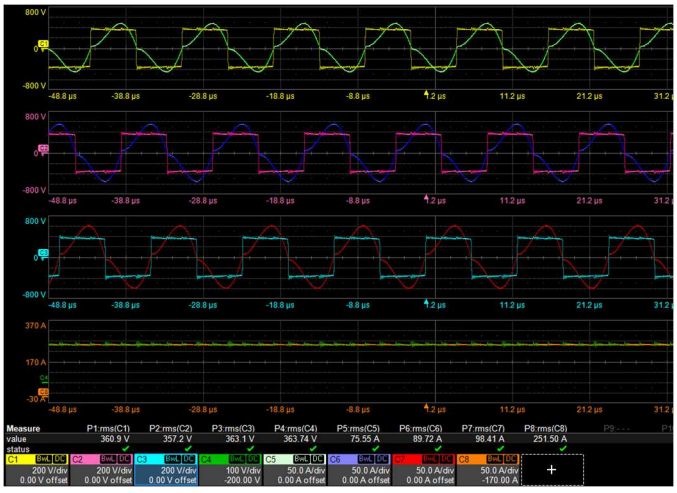

(b)

Fig. 8. Operational waveforms of the proposed system; inverter input dc and phase A, B, C voltages and currents and the rectifier input X, Y, Z and output dc voltages and currents.

IV. Conclusions

This study presents a 100-kW rated wireless power transfer system using polyphase electromagnetic couplers that have significantly higher surface and volumetric power densities compared to existing designs. The prototype development is validated for up to 90.6 kW as of now with an overall dc-to-dc efficiency of 90.83% and then inverter output -to- rectifier input efficiency of 97.4%. Future work will evaluate the inverter performance improvement with a modified resonant tuning network for a 'close to unity' resonant voltage gain as well as slight modifications on the resonant tuning inductors of the LCC network on primary-side to achieve more balanced inverter output currents.

Acknowledgment

This research used the resources available at the Power Electronics and Electric Machinery Research Center at the National Transportation Research Center, a US Department of Energy (DOE) Office of Energy Efficiency and Renewable Energy user facility operated by the Oak Ridge National Laboratory (ORNL). The authors would like to thank Dr. Burak Ozpineci (ORNL) and Dr. David E. Smith for their managerial support and technical guidance and Lee Slezak (DOE) for funding this work and project guidance.

References

[1] G. A. Covic and J. T. Boys, "Modern trends in inductive power transfer for transportation applications," *IEEE Journal of Emerging and Selected Topics Power Electronics*, vol. 1, no. 1, pp. 28–41, Mar. 2013.

[2] H. Feng, R. Tavakoli, O. C. Onar, and Z. Pantic, "Advances in high-power wireless charging systems: Overview and Design Considerations," *IEEE Transactions on Transportation Electrification*, vol. 6, no. 3, pp. 886-919, Sept. 2020.

[3] A. Foote and O. C. Onar, "A review of high-power wireless power transfer," in *Proc., IEEE Transportation Electrification Conference and Exposition (ITEC)*, pp. 234-240, June 2017, Chicago, IL.

[4] O. C. Onar, M. Chinthavali, S. Campbell, P. Ning, C. P. White, and J. M. Miller, "A SiC MOSFET based inverter for wireless power transfer applications," in *Proc., IEEE Applied Power Electronics Conference and Exposition (APEC)*, pp. 1690-1696, March 2014, Fort Worth, TX.

[5] M. S. Chinthavali, O. C. Onar, J. M. Miller and L. Tang, "Single-phase active boost rectifier with power factor correction for Wireless Power Transfer applications," *in Proc., IEEE Energy Conversion Congress and Exposition*, pp. 3258-3265, Sept. 2013, Denver, CO.

[6] O. C. Onar, M. Chinthavali, S. L. Campbell, L. E. Seiber, C. P. White, and and V. P. Galigekere, "Modeling, simulation, and experimental verification of a 20-kW series-series wireless power transfer system for a Toyota RAV4 electric vehicle," in *Proc., IEEE Transportation Electrification Conference and Expo (ITEC)*, pp. 874-880, June 2018, Long Beach, CA.

[7] J. Pries, V. P. Galigekere, O. C. Onar, G. -J. Su, R. Wiles, L. Seiber, J. Wilkins, S. Anwar, and S. Zou, "Coil power density optimization and trade-off study for a 100kW electric vehicle IPT wireless charging system," in *Proc., IEEE Energy Conversion Congress and Exposition (ECCE)*, pp. 1196-1201, September 2018, Portland, OR.

[8] V. P. Galigekere, J. Pries, O. C. Onar, G. -J. Su, S. Anwar, R. Wiles, L. Seiber, and J. Wilkins, "Design and implementation of an optimized 100 kW stationary wireless charging system for EV battery recharging," in *Proc., IEEE Energy Conversion Congress and Exposition (ECCE)*, pp. 3587-3592, September 2018, Portland, OR.

[9] J. M. Miller, A. W. Daga, F. J. McMahon, P. C. Schrafel, B. Cohen, and A. W. Calabro, "A closely coupled and scalable high power modular inductive charging system for vehicles," *IEEE Journal of Emerging and Selected Topics in Power Electronics (early access)*.

[10] R. Bosshard, U. Iruretagoyena, and J. W. Kolar, "Comprehensive evaluation of rectangular and double-D coil geometry for 50 kW/85 kHz IPT system," *IEEE Journal of Emerging and Selected Topics in Power Electronics*, vol. 4, no. 4, pp. 1406-1415, December 2016.

[11] S. Kim, G. A. Covic, and J. T. Boys, "Comparison of tripolar and circular pads for IPT charging systems," *IEEE Transactions on Power Electronics*, vol. 33, no. 7, pp. 6093-6103, July 2018.

[12] Y. Shiihara, R. Nagata, Y. Igawa, K. Okabe, H. Matsumoto, Y. Shibako, and Y. Neba, "Three-phase contactless power transformer with magnet yoke," in *Proc., 19th International Conference on Electrical Machines and Systems,* pp. 1-4, November 2016, Japan.

[13] D. J. Thrimawithana and U. K. Madawala, "A three-phase bi-directional IPT system for contactless charging of electric vehicles," in Proc., *IEEE International Symposium on Industrial Electronics*, pp. 1957-1962, June 2011, Poland.

[14] Y. Song, U. K. Madawala, T. Duleepa J, and A. P. Hu, "Cross coupling effects of poly-phase bi-directional inductive power transfer systems used for EV charging," in *Proc., IEEE 2nd International Future Energy Electronics Conference (IFEEC)*, pp. 1–7, November 2015, Taiwan.

[15] Y. Song, U. K. Madawala, D. J. Thrimawithana, and A. P. Hu, "LCL and CL compensations for wireless three phase bi-directional EV charging systems," in *Proc. IEEE 2nd Annual Southern Power Electronics Conference*, pp. 1–6, December 2016, Auckland, New Zealand.

[16] S. Kim, G. A. Covic, and J. T. Boys, "Tripolar pad for inductive power transfer systems for EV charging," *IEEE Transactions on Power Electronics*, vol. 32, no. 7, pp. 5045–5057, July 2017.

[17] D. J. Thrimawithana, U. K. Madawala, A. Francis, and M. Neath, "Magnetic modeling of a high-power three phase bi-directional IPT system," in *Proc., 37th Annual Conference of IEEE Industrial Electronincs Society*, pp. 1414–1419, November 2011, Melbourne, Australia.

[18] K. Kusaka, R. Kusui, J. -i. Itoh, D. Sato, S. Obayashi, and M. Ishida, "A 22 kW-85 kHz Three-phase Wireless Power Transfer System with 12 coils," in *Proc., IEEE Energy Conversion Congress and Exposition (ECCE)*, pp. 3340-3347, Sept.-Oct. 2019, Baltimore, MD.

[19] M. Mohammad, J. L. Pries, O. C. Onar, V. P. Galigekere, G. -J. Su, and J. Wilkins, "Three-phase LCC-LCC compensated 50-kW wireless charging system with non-zero interphase coupling," in *Proc., IEEE Applied Power Electronics Conference and Exposition (APEC)*, pp. 456-462, June 2021, Phoenix, AZ.

[20] J. Pries, V. P. N. Galigekere, O. C. Onar, and G. -J. Su, "A 50-kW three-phase wireless power transfer system using bipolar windings and series networks for rotating magnetic fields," *IEEE Transactions on Power Electronics*, vol. 35, no. 5, pp. 4500-4517, May 2020.

[21] R. Zeng, O. C. Onar, M. Mohammad, G. -J. Su, E. Asa, and V. P. Galigekere, "Modeling and analysis of a polyphase wireless power transfer system for EV charging applications," in *Proc., IEEE Applied Power Electronics Conference and Exposition*, March 2022, Houston, TX.